Nonlocal formulation of spin Coulomb drag

I. D'Amico[1] and C. A. Ullrich[2]
[1]*Department of Physics, University of York, York YO10 5DD, United Kingdom*
[2]*Department of Physics and Astronomy, University of Missouri–Columbia, Columbia, Missouri 65211, USA*
(Received 19 June 2013; revised manuscript received 13 October 2013; published 28 October 2013)

The spin Coulomb drag (SCD) effect occurs in materials and devices where charged carriers with different spins exchange momentum via Coulomb scattering. This causes frictional forces between spin-dependent currents that lead to intrinsic dissipation, which may limit spintronics applications. A nonlocal formulation of SCD is developed which is valid for strongly inhomogeneous systems such as nanoscale spintronics devices. This nonlocal formulation of SCD is successfully applied to linewidths of intersubband spin plasmons in semiconductor quantum wells, where experiments have shown that the local approximation fails.

DOI: 10.1103/PhysRevB.88.155324 PACS number(s): 72.25.Rb, 31.15.ee, 73.21.−b, 85.75.−d

I. INTRODUCTION

The performance of nanoscale electronic devices is limited by dissipative effects. There are many possible sources of dissipation: some of them can be controlled, for example by reducing disorder, whereas others are intrinsic and hence unavoidable. One such relaxation mechanism is the spin Coulomb drag (SCD),[1,2] which plays an important role in spintronics.[3,4] The SCD effect occurs when two different spin populations move with different momentum while interacting via Coulomb scattering. The exchange of momentum leads to a drag force between the two spin populations which causes a decay—and eventually a halting—of spin currents. On the other hand, SCD favors coherent transport of spin packets in semiconductors by strongly decreasing the spin-diffusion coefficients with respect to the charge ones, while maintaining the high electron mobility.[5–8]

The standard phenomenological way of introducing the SCD is by considering a homogeneous system in which two populations of spin-σ and spin-$\bar{\sigma}$ electrons, with densities n_σ and $n_{\bar{\sigma}}$, are moving with velocities $\mathbf{v}_\sigma(t) = \mathbf{v}_\sigma e^{-i\omega t}$ and $\mathbf{v}_{\bar{\sigma}}(t) = \mathbf{v}_{\bar{\sigma}} e^{-i\omega t}$. The spin-$\bar{\sigma}$ population exerts a Coulomb force per unit volume

$$\mathbf{F}_{\sigma\bar{\sigma}}(\omega) = e^2 n_\sigma n_{\bar{\sigma}} \mathrm{Re}\, \rho^{\mathrm{hom}}_{\sigma\bar{\sigma}}(\omega, n_\sigma, n_{\bar{\sigma}})(\mathbf{v}_\sigma - \mathbf{v}_{\bar{\sigma}}) \qquad (1)$$

on the spin-σ electrons. The frequency-dependent spin transresistivity of a homogeneous system,[1] $\rho^{\mathrm{hom}}_{\sigma\bar{\sigma}}(\omega, n_\sigma, n_{\bar{\sigma}})$, is a measure of the SCD. The resulting power loss density for the σ-spin population is given by $P_\sigma(\omega, n_\uparrow, n_\downarrow) = \mathbf{F}_{\sigma\bar{\sigma}} \cdot \mathbf{v}_\sigma$. The total SCD power loss for spin-σ electrons in an inhomogeneous system can then be obtained using a local approximation.[9]

However, such a description becomes questionable[10] when considering nanoscale systems, where interfaces, quantum confinement, or local doping can lead to strong inhomogeneities of background densities as well as current distributions. In this paper we develop a formalism for the SCD valid in the general inhomogeneous case, and we demonstrate for the damping of spin plasmons in quantum wells that it is superior to the local approximation.

II. MICROSCOPIC DERIVATION OF THE NONLOCAL SPIN TRANSRESISTIVITY

To generalize Eq. (1) we consider the microscopic force that a volume element of spin-$\bar{\sigma}$ at position $\mathbf{r}'$ with velocity $\mathbf{v}_{\bar{\sigma}}(\mathbf{r}')$ exerts on a volume element of spin-σ at position $\mathbf{r}$ with velocity $\mathbf{v}_\sigma(\mathbf{r})$ (see Fig. 1):

$$\mathbf{F}_{\sigma\bar{\sigma}}(\mathbf{r},\mathbf{r}',\omega) = e^2 n_\sigma(\mathbf{r}) n_{\bar{\sigma}}(\mathbf{r}') \mathrm{Re}\, \overleftrightarrow{\rho}_{\sigma\bar{\sigma}}(\mathbf{r},\mathbf{r}',\omega)[\mathbf{v}_\sigma(\mathbf{r}) - \mathbf{v}_{\bar{\sigma}}(\mathbf{r}')], \qquad (2)$$

where $\overleftrightarrow{\rho}_{\sigma\bar{\sigma}}(\mathbf{r},\mathbf{r}',\omega)$ is the nonlocal spin-transresistivity tensor. The total SCD power loss of spin-σ electrons in an inhomogeneous system will then be given by

$$\bar{P}_\sigma(\omega) = e^2 \int d^3r \int d^3r'\, n_\sigma(\mathbf{r}) n_{\bar{\sigma}}(\mathbf{r}') \times \mathbf{v}_\sigma(\mathbf{r}) \cdot \{\mathrm{Re}\, \overleftrightarrow{\rho}_{\sigma\bar{\sigma}}(\mathbf{r},\mathbf{r}',\omega)[\mathbf{v}_\sigma(\mathbf{r}) - \mathbf{v}_{\bar{\sigma}}(\mathbf{r}')]\}. \qquad (3)$$

The major task is to evaluate the nonlocal spin-transresistivity tensor. To do this, we start with the Kubo formula for the spin-current response tensor in inhomogeneous systems,[12]

$$\sigma^{\alpha\beta}_{\sigma\sigma'}(\mathbf{r},\mathbf{r}',\omega) = \frac{ie^2}{m\omega}\left[n_\sigma(\mathbf{r})\delta(\mathbf{r}-\mathbf{r}')\delta_{\sigma\sigma'}\delta_{\alpha\beta} + m\left\langle\left\langle J^\alpha_\sigma(\mathbf{r}); J^\beta_{\sigma'}(\mathbf{r}')\right\rangle\right\rangle_\omega\right], \qquad (4)$$

where $J^\alpha_\sigma(\mathbf{r})$ is the total spin-current operator for spin σ, defined as

$$J^\alpha_\sigma(\mathbf{r}) = \frac{1}{2m}\sum_i^{N_\sigma}\left[p^\alpha_i \delta(\mathbf{r}-\mathbf{r}_i) + \delta(\mathbf{r}-\mathbf{r}_i)p^\alpha_i\right], \qquad (5)$$

$p^\alpha_i = -i\hbar\nabla_\alpha$, and α and β are Cartesian coordinates. $\langle\langle A; B\rangle\rangle_\omega$ denotes the standard frequency-dependent response function for the operators A and B.[12] By inverting the Kubo formula to first order in the response function (which is sufficient since we are working in linear-response theory), we find

$$\rho^{\alpha\beta}_{\sigma\bar{\sigma}}(\mathbf{r},\mathbf{r}',\omega) = \frac{i\omega m^2}{e^2}\frac{\left\langle\left\langle J^\alpha_\sigma(\mathbf{r}); J^\beta_{\bar{\sigma}}(\mathbf{r}')\right\rangle\right\rangle_\omega}{n_\sigma(\mathbf{r})n_{\bar{\sigma}}(\mathbf{r}')}. \qquad (6)$$

In the next step, we twice apply the equation of motion $\langle\langle A; B\rangle\rangle_\omega = \omega^{-1}(\langle[A,B]\rangle + i\langle\langle\dot{A}; B\rangle\rangle_\omega)$, where $\dot{A} = -(i/\hbar)[A,H]$, and $H = T + W_{\mathrm{Coul}} + V_{\mathrm{ext}}$ is the many-body Hamiltonian of the system (kinetic energy plus Coulomb interaction plus external potential).

For the real part of the nonlocal spin transresistivity, the dominant contribution from Coulomb interaction (and to the

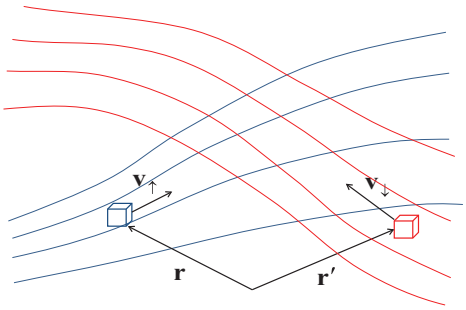

FIG. 1. (Color online) Schematic illustration of two volume elements of inhomogeneous spin-up and spin-down electron velocity distributions, indicated by blue and red streamlines, respectively. The volume elements interact via Coulomb forces; the resulting exchange of momentum leads to the SCD effect.

SCD) is then given by

$$\left[\mathrm{Re}\rho^{\alpha\beta}_{\sigma\bar{\sigma}}(\mathbf{r},\mathbf{r}',\omega)\right]_{\mathrm{SCD}} = \frac{m^2}{\omega e^2}\frac{\mathrm{Im}\left\langle\!\left\langle j^{\alpha}_{\sigma,\mathrm{Coul}}(\mathbf{r});\, j^{\beta}_{\bar{\sigma},\mathrm{Coul}}(\mathbf{r}')\right\rangle\!\right\rangle_{\omega}}{n_{\sigma}(\mathbf{r})n_{\bar{\sigma}}(\mathbf{r}')}, \tag{7}$$

where

$$j^{\alpha}_{\sigma,\mathrm{Coul}}(\mathbf{r}) = -\frac{i}{\hbar}\left[J^{\alpha}_{\sigma}, W_{\mathrm{Coul}}\right] \tag{8}$$

$$= -\frac{e^2}{mV^2}\sum_{\mathbf{q}} v_q \rho_{-\mathbf{q}\bar{\sigma}} q^{\alpha} \sum_{\mathbf{q}'} e^{i\mathbf{q}'\cdot\mathbf{r}}\rho_{(\mathbf{q}-\mathbf{q}')\sigma}. \tag{9}$$

Here, $v_q = 4\pi/q^2$ is the Fourier transform of the Coulomb interaction, $\rho_{\mathbf{q}\sigma} = \sum_k^{N_\sigma} e^{i\mathbf{q}\cdot\mathbf{r}_k}$ is the density fluctuation operator, and V is the volume. The real part of the spin transresistivity (omitting the label SCD) then follows as

$$\mathrm{Re}\rho^{\alpha\beta}_{\sigma\bar{\sigma}}(\mathbf{r},\mathbf{r}',\omega) = \frac{e^2}{\omega V^4}\frac{1}{n_{\sigma}(\mathbf{r})n_{\bar{\sigma}}(\mathbf{r}')}\sum_{\mathbf{q}\mathbf{q}'} v_q v_{q'} q^{\alpha} q'^{\beta}\,\mathrm{Im}\sum_{\mathbf{q}''\mathbf{q}'''} e^{i\mathbf{q}''\cdot\mathbf{r}} e^{i\mathbf{q}'''\cdot\mathbf{r}'}\left\langle\!\left\langle \rho_{-\mathbf{q}\bar{\sigma}}\rho_{(\mathbf{q}-\mathbf{q}'')\sigma};\, \rho_{-\mathbf{q}'\sigma}\rho_{(\mathbf{q}'-\mathbf{q}''')\bar{\sigma}}\right\rangle\!\right\rangle_{\omega}. \tag{10}$$

It is not difficult to see that the four-point function $\langle\langle \rho_{-\mathbf{q}\bar{\sigma}}\rho_{(\mathbf{q}-\mathbf{q}'')\sigma};\, \rho_{-\mathbf{q}'\sigma}\rho_{(\mathbf{q}'-\mathbf{q}''')\bar{\sigma}}\rangle\rangle_{\omega}$ is even under the simultaneous inversion of all momenta, $\mathbf{q},\mathbf{q}',\mathbf{q}'',\mathbf{q}''' \longrightarrow -\mathbf{q}, -\mathbf{q}', -\mathbf{q}'', -\mathbf{q}'''$. We can therefore rewrite Eq. (10) as

$$\mathrm{Re}\rho^{\alpha\beta}_{\sigma\bar{\sigma}}(\mathbf{r},\mathbf{r}',\omega) = \frac{e^2}{\omega V^4}\frac{1}{n_{\sigma}(\mathbf{r})n_{\bar{\sigma}}(\mathbf{r}')}\sum_{\mathbf{q}\mathbf{q}'} v_q v_{q'} q^{\alpha} q'^{\beta}\sum_{\mathbf{q}''\mathbf{q}'''} e^{i\mathbf{q}''\cdot\mathbf{r}} e^{i\mathbf{q}'''\cdot\mathbf{r}'}\mathrm{Im}\left\langle\!\left\langle \rho_{\mathbf{q}\bar{\sigma}}\rho_{(\mathbf{q}''-\mathbf{q})\sigma};\, \rho_{\mathbf{q}'\sigma}\rho_{(\mathbf{q}'''-\mathbf{q}')\bar{\sigma}}\right\rangle\!\right\rangle_{\omega}, \tag{11}$$

where the imaginary part refers only to the four-point function $\langle\langle \rho_{\mathbf{q}\bar{\sigma}}\rho_{(\mathbf{q}''-\mathbf{q})\sigma};\, \rho_{\mathbf{q}'\sigma}\rho_{(\mathbf{q}'''-\mathbf{q}')\bar{\sigma}}\rangle\rangle_{\omega}$. Equation (11) is completely general and formally exact.

The final step is to evaluate the four-point function. Here we focus on the zero-temperature limit, and use the decoupling approximation of Ref. 13; we thus obtain the following key result:

$$\begin{aligned}\mathrm{Re}\rho^{\alpha\beta}_{\sigma\bar{\sigma}}(\mathbf{r},\mathbf{r}',\omega) \approx \frac{\hbar e^2}{\omega V^4}\frac{1}{n_{\sigma}(\mathbf{r})n_{\bar{\sigma}}(\mathbf{r}')}\sum_{\mathbf{q}\mathbf{q}'} v_q v_{q'} q^{\alpha} q'^{\beta}\sum_{\mathbf{q}''\mathbf{q}'''} e^{i\mathbf{q}''\cdot\mathbf{r}} e^{i\mathbf{q}'''\cdot\mathbf{r}'}\int_0^{\omega}\frac{d\omega'}{\pi}\Big\{&\mathrm{Im}\chi^{\mathrm{RPA}}_{\bar{\sigma}\sigma}(\mathbf{q},\mathbf{q}',\omega')\mathrm{Im}\chi^{\mathrm{RPA}}_{\sigma\bar{\sigma}}(\mathbf{q}''-\mathbf{q},\mathbf{q}'''-\mathbf{q}',\omega-\omega')\\ &+\mathrm{Im}\chi^{\mathrm{RPA}}_{\bar{\sigma}\bar{\sigma}}(\mathbf{q},\mathbf{q}'''-\mathbf{q}',\omega')\mathrm{Im}\,\chi^{\mathrm{RPA}}_{\sigma\sigma}(\mathbf{q}''-\mathbf{q},\mathbf{q}',\omega-\omega')\Big\},\end{aligned} \tag{12}$$

where $\mathrm{Im}\chi^{\mathrm{RPA}}_{\bar{\sigma}\sigma}$ is the imaginary part of the spin-resolved density-density response function in the random phase approximation (RPA). Substituting expression (12) into Eq. (3) allows us to calculate the dissipation due to the SCD explicitly for any inhomogeneous system.

It is instructive to derive the homogeneous limit of this expression, where the spin densities n_σ and $n_{\bar{\sigma}}$ become constant. We write Eq. (12) as the Fourier transform

$$\mathrm{Re}\rho^{\alpha\beta}_{\sigma\bar{\sigma}}(\mathbf{r},\mathbf{r}',\omega) = \frac{1}{V^2}\sum_{\mathbf{q}''}\sum_{\mathbf{q}'''} e^{i\mathbf{q}\cdot\mathbf{r}} e^{i\mathbf{q}''\cdot\mathbf{r}'''}\mathrm{Re}\rho^{\alpha\beta}_{\sigma\bar{\sigma}}(\mathbf{q}'',\mathbf{q}''',\omega). \tag{13}$$

In the homogeneous limit, all RPA response functions are written as $\mathrm{Im}\chi^{\mathrm{RPA}}_{\bar{\sigma}\sigma}(\mathbf{q},\mathbf{q}',\omega')\delta_{\mathbf{q},\mathbf{q}'} = V\mathrm{Im}\chi^{\mathrm{RPA}}_{\bar{\sigma}\sigma}(\mathbf{q},\omega')\delta_{\mathbf{q},\mathbf{q}'}$ [and similarly for all other RPA response functions in Eq. (12)], so that $\mathrm{Re}\rho^{\alpha\beta}_{\sigma\bar{\sigma}}(\mathbf{q}'',\mathbf{q}''',\omega)$ becomes diagonal in $\mathbf{q}''$ and $\mathbf{q}'''$. The homogeneous limit of the spin transresistivity is then given by its $\mathbf{q}'' = 0$ component, and we obtain

$$\begin{aligned}\left[\mathrm{Re}\rho^{\alpha\beta}_{\sigma\bar{\sigma}}(\omega)\right]_{\mathrm{hom}} = \frac{\hbar e^2}{\omega V}\frac{1}{n_{\sigma}n_{\bar{\sigma}}}\sum_{\mathbf{q}} v_q^2 q^{\alpha} q^{\beta}\int_0^{\omega}\frac{d\omega'}{\pi}&\\ \times\Big\{\mathrm{Im}\chi^{\mathrm{RPA}}_{\bar{\sigma}\sigma}(q,\omega')\mathrm{Im}\chi^{\mathrm{RPA}}_{\sigma\bar{\sigma}}(q,\omega-\omega')&\\ -\mathrm{Im}\chi^{\mathrm{RPA}}_{\bar{\sigma}\bar{\sigma}}(q,\omega')\mathrm{Im}\chi^{\mathrm{RPA}}_{\sigma\sigma}(q,\omega-\omega')\Big\}.&\end{aligned} \tag{14}$$

The trace of this gives the zero-temperature limit of the homogeneous spin transresistivity of Ref. 1: $(1/3)\sum_{\alpha}[\mathrm{Re}\rho^{\alpha\alpha}_{\sigma\bar{\sigma}}(\omega)]_{\mathrm{hom}} = \mathrm{Re}\rho_{\sigma\bar{\sigma}}(\omega, T=0)$.

III. APPLICATION: INTRINSIC DISSIPATION OF INTERSUBBAND SPIN PLASMONS

We now test this general formalism for a quantum well geometry, where the breakdown of the local approximation can be clearly illustrated. Spin plasmons in quantum wells[14,15] offer intriguing ways of studying the spin dynamics of interacting electrons in semiconductors. The SCD gives an

intrinsic contribution to the spin-plasmon linewidth[9] which cannot be avoided even in systems without any disorder. This provides sensitive tests for first-principles descriptions of the SCD.

In Ref. 9, the spin-plasmon linewidth was calculated within a linear response formalism[16,17] in which the SCD was treated using a local approximation. However, in a recent experimental study of intersubband spin plasmons using inelastic light scattering,[15] it was found that the local formalism from Ref. 9, although giving the right order of magnitude, significantly overestimates the actual spin-plasmon linewidth. As we will show, the failure of the local approximation is related to the crossover between two-dimensional (2D) and three-dimensional (3D) behavior of the intersubband dynamics in quantum wells.

We consider the dynamics of conduction electrons in n-doped GaAs/AlGaAs quantum wells with given sheet density N_s.[18] The quantum well is assumed to be nonmagnetic, i.e., there is an equal number of spin-up and spin-down electrons. We assume the electronic single-particle states to be plane waves in the x-y plane of the well, and quantized along the z direction. In the effective-mass approximation, the subband envelope functions follow from a one-dimensional Kohn-Sham equation,[19]

$$\left[-\frac{\hbar^2}{2m^*}\frac{d^2}{dz^2}+v_{\rm conf}(z)+v_{\rm H}(z)+v_{\rm xc}(z)\right]\varphi_j(z)=\varepsilon_j\varphi_j(z), \tag{15}$$

where m^* is the effective mass (for simplicity we assume the same m^* in well and barrier). Here, $v_{\rm conf}$ is the quantum well confining potential, $v_{\rm H}$ is the Hartree potential, and $v_{\rm xc}$ is the exchange-correlation (xc) potential, which we approximate using the 3D local-density approximation (LDA). As shown by Pollack and Perdew,[20] the 3D LDA is appropriate for the ground-state electronic structure of sufficiently wide quantum wells, such as the systems we will consider here. Furthermore, we ignore spin-orbit interactions.

Equation (15) describes parabolic subbands with envelope functions $\varphi_j(z)$ and energies $\varepsilon_j+\hbar^2k_{||}^2/2m^*$, where $\mathbf{k}_{||}$ is the in-plane wave vector. We assume that only the lowest subband is occupied, up to the conduction-band Fermi energy $\varepsilon_{\rm F}=\varepsilon_1+\pi N_s\hbar^2/m^*$.[18,19]

The single-particle and collective excitations are obtained from time-dependent density-functional theory in linear response,[21] using the adiabatic LDA. Figure 2 shows the intra- and intersubband excitation spectra, indicating the particle-hole continuum regions and the intersubband charge- and spin-plasmon frequency dispersions $\Omega_c(\mathbf{q}_{||})$ and $\Omega_s(\mathbf{q}_{||})$, where $\mathbf{q}_{||}$ is the in-plane plasmon wave vector; we here assume isotropy in the plane, so the plasmon dispersions depend only on the magnitude $q_{||}$ of the wave vector. In an unmagnetized bulk system there would be only a charge plasmon but no spin plasmon; this is because the particle-hole continuum of the 3D electron gas is gapless. Similarly, there is no intrasubband spin plasmon in an unmagnetized 2D electron gas.[22]

From a dynamical point of view, the intersubband plasmons are collective oscillations of the electrons in the quantum well: in a charge plasmon, the spin-up and spin-down electrons oscillate in phase; in the spin plasmon they oscillate with

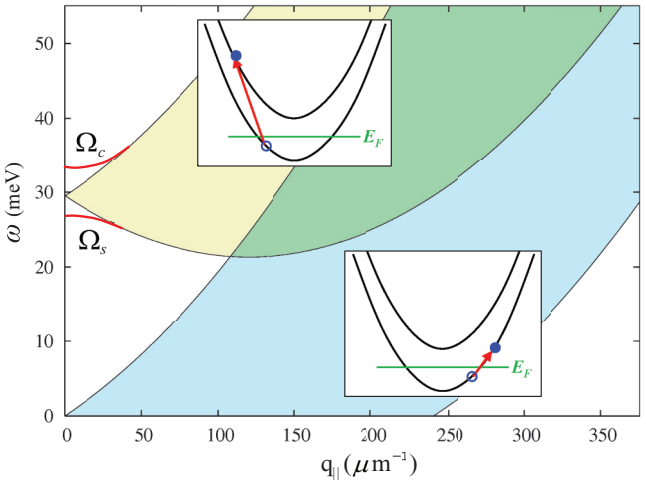

FIG. 2. (Color online) Electronic excitations in a 20-nm n-doped quantum well with $N_s=2.3\times10^{11}$ cm^{-2} (Ref. 15). The intrasubband and first intersubband particle-hole (p-h) continua are shaded in light blue and yellow, respectively; the charge and spin plasmon dispersions are indicated by Ω_c and Ω_s. The two insets show a pair of inter- and intrasubband p-h excitations, respectively, which form the dominant spin-plasmon decay channel.

opposite phase. The associated currents flow back and forth along the z direction. We can express the time-dependent spin-up and -down current densities of the two plasmons as follows:

$$\mathbf{j}^c_{\uparrow,\downarrow}(\mathbf{q}_{||},z,t)=j_c(q_{||},z)\hat{z}\,e^{-i\Omega_c(q_{||})t}, \tag{16}$$

$$\mathbf{j}^s_{\uparrow,\downarrow}(\mathbf{q}_{||},z,t)=j_s(q_{||},z)\hat{z}\,e^{-i[\Omega_s(q_{||})t\pm\pi/2]}, \tag{17}$$

where $\hat{z}$ is a unit vector along the z axis. We have used here a mixed $(\mathbf{q}_{||},z)$ representation, defined via a Fourier transformation over the in-plane coordinates $\mathbf{r}_{||}=(x,y)$, which accounts for the fact that the system is homogeneous in the plane and quantum confined along z. In the following we will limit the discussion to the case $q_{||}=0$. This results in technical simplifications, and it is justified as in practice the plasmon wave vectors are rather small (see Fig. 2), so the plasmon linewidth at zero $q_{||}$ will not differ much from the linewidth at the finite values of $q_{||}$ considered experimentally.

In the two-level approximation, the charge and spin plasmons have the same velocity field $v_{12}(z)=j_{c,s}(z)/n_\sigma(z)$, given by

$$v_{12}(z)=\frac{\hbar}{m^*n_\sigma(z)}\left[\varphi_2(z)\frac{d}{dz}\varphi_1(z)-\varphi_1(z)\frac{d}{dz}\varphi_2(z)\right], \tag{18}$$

where $n_\sigma(z)=n_{\bar\sigma}(z)=n(z)/2$. In Ref. 9 we derived, within the framework of time-dependent spin-current density functional theory, the following expression[23] for the SCD linewidth of the spin plasmon at $q_{||}=0$:

$$\Gamma^{\rm loc}_{\rm SCD}=\frac{e^2N_s}{4\Omega_s}\int dz\,{\rm Re}\rho^{\rm hom}_{\uparrow\downarrow}(\Omega_s;n_\uparrow(z),n_\downarrow(z))v_{12}^2(z)n^2(z). \tag{19}$$

Equation (19) is physically very appealing: its structure reflects the SCD power loss derived phenomenologically from Eq. (1),

TABLE I. Experimental and calculated spin-plasmon linewidths (in meV) for two different quantum well samples.

	$2\Gamma_{\rm expt}$	$2\Gamma^{\rm loc}_{\rm SCD}$	$2\Gamma^{\rm nloc}_{\rm SCD}$	$2\Gamma^{\rm nloc}_{\rm SCD}+{\rm xc}$
Sample 1 (Ref. 14)[a]	0.16	0.40	0.014	0.015
Sample 2 (Ref. 15)[b]	0.12	0.40	0.020	0.021

[a]Width 25 nm, $N_s = 1.6\times10^{11}$ cm^{-2}, $\mu = 1.1\times10^{6}$ cm^2/V s.
[b]Width 20 nm, $N_s = 2.3\times10^{11}$ cm^{-2}, $\mu = 2\times10^{7}$ cm^2/V s.

and suggests a simple, local, Ohmic-like dissipation of the spin currents.

$\Gamma^{\rm loc}_{\rm SCD}$ can be compared to experimental results for quantum wells from inelastic light scattering.[14,15] $2\Gamma_{\rm SCD}$ is the SCD contribution to the full width at half maximum of the spin-plasmon peak; from Table I we see that the local approximation overestimates the linewidth by a factor of 2–3 in two different systems.

The overdamping of the local approximation (19) suggests that a different approach is needed: the local approximation may be underestimating the effect of inhomogeneities while its use of a homogeneous 3D system as reference frame implies that quantization along the growth axis is not properly taken into account. Thus, the SCD linewidth of intersubband spin plasmons needs to be generalized to a nonlocal form which fully accounts for inhomogeneity and quantization.

To do so, we use our general formalism for the inhomogeneous spin transresistivity presented above to calculate the spin-plasmon linewidth. By comparison with Eq. (3), and using a mixed $(\mathbf{q}_{||},z)$ representation, we obtain

$$\Gamma^{\rm nloc}_{\rm SCD} = \frac{e^2N_s}{2m^*\Omega_s}\int dz\int dz'{\rm Re}\rho^{zz}_{\uparrow\downarrow}(\mathbf{q}_{||}=0,z,z',\Omega_s) \times n_\sigma(z)n_{\bar\sigma}(z')\left[v^2_{12}(z)+v_{12}(z)v_{12}(z')\right]. \quad (20)$$

Notice that here we need only the zz component of the spin-transresistivity tensor ${\rm Re}\overleftrightarrow{\rho}_{\sigma\bar\sigma}$, because the currents associated with the plasmon are along the z direction. The main task is to obtain ${\rm Re}\rho^{zz}_{\uparrow\downarrow}(\mathbf{q}_{||}=0,z,z',\omega)$ from Eq. (12) by Fourier transformation with respect to the in-plane coordinates. The calculation is aided by momentum conservation due to the homogeneity in the quantum well plane, which can be accounted for in Eq. (12) by multiplying the RPA response functions with δ functions: for instance, ${\rm Im}\chi^{\rm RPA}_{\bar\sigma\sigma}(\mathbf{q},\mathbf{q}',\omega')\delta_{\mathbf{q}_{||}-\mathbf{q}'_{||}}$, and similarly for all RPA response functions. Furthermore, we express the Coulomb interaction as

$$v_q = \int dz\, e^{iq_zz}v^{\rm 2D}_{q_{||}}e^{-q_{||}|z|}, \quad (21)$$

where $v^{\rm 2D}_q = 2\pi/q_{||}$ is the 2D Coulomb interaction. After lengthy but straightforward manipulations, we obtain

$$\Gamma^{\rm nloc}_{\rm SCD} = \frac{e^4\hbar}{2m^{*2}V^2}\frac{N_s}{\Omega_s^2}\int dz\int dz'\left[v^2_{12}(z)+v_{12}(z)v_{12}(z')\right]\sum_{\mathbf{q}_{||}}\left(v^{\rm 2D}_{q_{||}}\right)^2q^2_{||}\int_0^\omega\frac{d\omega'}{\pi}\int ds_1\int ds_2\,{\rm sgn}(z-s_1)\,e^{-q_{||}|z-s_1|}\,{\rm sgn}(z'-s_2) \times e^{-q_{||}|z'-s_2|}\left\{{\rm Im}\chi^{\rm RPA}_{\bar\sigma\sigma}(\mathbf{q}_{||},s_1,s_2,\omega'){\rm Im}\chi^{\rm RPA}_{\sigma\bar\sigma}(-\mathbf{q}_{||},z,z',\omega-\omega') + {\rm Im}\chi^{\rm RPA}_{\bar\sigma\bar\sigma}(\mathbf{q}_{||},s_1,z',\omega'){\rm Im}\chi^{\rm RPA}_{\sigma\sigma}(-\mathbf{q}_{||},z,s_2,\omega-\omega')\right\}. \quad (22)$$

We have evaluated Eq. (22) for the two experimentally studied quantum wells; the results are given in Table I. It can be seen that $2\Gamma^{\rm nloc}_{\rm SCD}$ is now smaller than the experimental linewidth, as expected: the total linewidth will include extrinsic contributions from disorder, interface roughness, phonons, etc. in addition to the intrinsic SCD contribution. Indeed, sample 1 has the larger linewidth $2\Gamma_{\rm expt}$ mainly because of its smaller mobility μ (which indicates more disorder), in spite of the fact that the SCD contribution is smaller than in sample 2.

We also considered the impact of dynamical exchange-correlation (xc) effects beyond the RPA by replacing ${\rm Im}\chi^{\rm RPA}_{\sigma\sigma'}$ with ${\rm Im}\chi^{\rm RPA+xc}_{\sigma\sigma'}$ in Eq. (22), i.e., by including an xc local field factor. In contrast to the findings of Ref. 24 we observe only a slight increase of the SCD plasmon linewidth (see the rightmost column of Table I).

We will now discuss why the nonlocal approach successfully reduces the spin-plasmon linewidth. Let us first look at the structure of Eq. (22). The RPA response function matrix is defined as $[\underline{\underline{\chi}}^{\rm RPA}]^{-1} = [\underline{\underline{\chi}}^{0}]^{-1} - \underline{\underline{f}}_{\rm H}$, where $f_{\rm H}$ is the Hartree kernel, and in mixed representation the quasi-2D noninteracting response function is

$$\chi^0_{\sigma\sigma'}(\mathbf{q}_{||},z,z',\omega) = \delta_{\sigma\sigma'}\sum_{j=1}^{\rm occ}\sum_{l=1}^{\infty}F_{lj}(\mathbf{q}_{||},\omega)\varphi_j(z)\varphi_l(z)\varphi_j(z')\varphi_l(z'). \quad (23)$$

$F_{lj}(\mathbf{q}_{||},\omega)$ has a form similar to a 2D Lindhard function, and defines a 2D particle-hole (p-h) continuum for each pair of subband indices l and j.[18,21] In contrast to the local approximation, $\chi^{\rm RPA}$, through Eq. (23), therefore explicitly accounts for the spectral information related to the quantization and strong inhomogeneity along the growth direction.

The intrinsic dissipation of the spin plasmons arises from a decay of the coherent plasmon mode (moving along z) into incoherent pairs of p-h excitations moving in the plane of the well. This can be explicitly seen already in Eq. (11) from the presence of the four-point function, which describes correlated pairs of p-h excitations.

However, the available continuum of p-h excitations strongly depends on the system. The *local* approximation assumes that, independent of the geometry of the system, the plasmon couples locally to a 3D continuum. By contrast, in a quantum well the continuum is restricted to the 2D in-plane direction, due to quantization. This creates a bottleneck for energy conservation, and hence reduces the plasmon linewidth.

The plasmon is a coherent superposition of intersubband p-h excitations. To dissipate its energy, it decays into incoherent p-h pairs; thus, the most efficient decay channel would be decay into two intersubband p-h pairs, i.e., $j=1$ and $l=2$ in Eq. (23). However, energy and momentum must be conserved: the two p-h pairs must have total energy ω and total in-plane momentum $q_{||}=0$. The energy conservation blocks the

intersubband-intersubband decay channel. The next possibility is one intrasubband and one intersubband ($j = l = 1$) p-h pair (see the insets in Fig. 2), which in fact turns out to be the dominant contribution to $\Gamma_{\mathrm{SCD}}^{\mathrm{nloc}}$.

IV. CONCLUSIONS

In this paper, we have derived a general nonlocal approach to SCD which is valid in inhomogeneous systems. This allows for a quantitatively accurate description of SCD in nanoscale device components. In particular, it tells us how collective excitations in nanostructures dissipate, which is of practical interest in areas such as plasmonics.[25]

The application explicitly discussed provides an unequivocal example of a breakdown of the local approximation in a situation in which there is a dimensionality crossover between 2D and 3D. The local approximation assumes a 3D homogeneous reference system: energy bottlenecks due to finite-size quantization are therefore not included. Our results show that to describe the SCD dissipation in nanoscale systems correctly, detailed spectral information is needed. In view of the immense popularity of local approximations in condensed-matter physics and other areas of science, these findings have important general implications for developing new ways for treating dynamical many-body effects in nanoscale systems.

For the quantum well systems that we discussed in the second part of the paper, the intrinsic SCD contribution to the spin-plasmon linewidth turned out to be significantly smaller compared to other, extrinsic dissipation mechanisms such as disorder or interface roughness. In principle, reducing the disorder and surface roughness in the system should eventually lead to situations where the SCD becomes the dominating mechanism; however, it is unclear whether this is practically feasible (the quantum wells under consideration in this paper are already very clean, as evidenced by their high mobility). A better approach to isolate the intrinsic SCD contribution to the linewidth may be to compare experimental data for the spin and charge intersubband plasmons for a parabolic quantum well, as we suggested in Ref. 9. Since intersubband charge plasmons in harmonically confined systems are protected from intrinsic dissipation due to electronic many-body effects,[26] comparing the charge- and spin-plasmon linewidths in the same parabolic well should provide a rather clear-cut experimental way to identify the intrinsic contributions to the spin-plasmon linewidth.

ACKNOWLEDGMENTS

We thank Florent Perez and Florent Baboux for valuable discussions. I.D'A. acknowledges support from EPSRC Grant No. EP/F016719/1 and from Royal Society Grant No. IJP 2008/R1 JP0870232. C.A.U. is supported by DOE Grant No. DE-FG02-05ER46213.

[1] I. D'Amico and G. Vignale, Phys. Rev. B **62**, 4853 (2000).
[2] I. D'Amico and C. A. Ullrich, Phys. Status Solidi B **247**, 235 (2010).
[3] I. Žutić, J. Fabian, and S. Das Sarma, Rev. Mod. Phys. **76**, 323 (2004).
[4] M. W. Wu, J. H. Jiang, and M. Q. Weng, Phys. Rep. **493**, 61 (2010).
[5] I. D'Amico and G. Vignale, Europhys. Lett. **55**, 566 (2001).
[6] I. D'Amico and G. Vignale, Phys. Rev. B **65**, 085109 (2002).
[7] C. P. Weber, N. Gedik, J. E. Moore, J. Orenstein, J. Stephens, and D. D. Awschalom, Nature (London) **437**, 1330 (2005).
[8] L. Yang, J. D. Koralek, J. Orenstein, D. R. Tibbetts, J. L. Reno, and M. P. Lilly, Nat. Phys. **8**, 153 (2012).
[9] I. D'Amico and C. A. Ullrich, Phys. Rev. B **74**, 121303(R) (2006).
[10] The local approximation for viscous damping of charge plasmons was the subject of a recent study (Ref. 11) using a perturbative approach, suggesting the need for better approximations to account for geometric confinement.
[11] R. D'Agosta, M. Di Ventra, and G. Vignale, Phys. Rev. B **76**, 035320 (2007).
[12] G. F. Giuliani and G. Vignale, *Quantum Theory of the Electron Liquid* (Cambridge University Press, Cambridge, 2005).
[13] R. Nifosì, S. Conti, and M. P. Tosi, Phys. Rev. B **58**, 12758 (1998).
[14] A. Pinczuk, S. Schmitt-Rink, G. Danan, J. P. Valladares, L. N. Pfeiffer, and K. W. West, Phys. Rev. Lett. **63**, 1633 (1989).
[15] F. Baboux, F. Perez, C. A. Ullrich, I. D'Amico, J. Gomez, and M. Bernard, Phys. Rev. Lett. **109**, 166401 (2012).
[16] Z. Qian, A. Constantinescu, and G. Vignale, Phys. Rev. Lett. **90**, 066402 (2003).
[17] Z. Qian and G. Vignale, Phys. Rev. B **68**, 195113 (2003).
[18] C. A. Ullrich and G. Vignale, Phys. Rev. B **58**, 15756 (1998).
[19] P. Harrison, *Quantum Wells, Wires and Dots*, 2nd ed. (Wiley, Chichester, 2005).
[20] L. Pollack and J. P. Perdew, J. Phys.: Condens. Matter **12**, 1239 (2000).
[21] C. A. Ullrich, *Time-Dependent Density-Functional Theory: Concepts and Applications* (Oxford University Press, Oxford, 2012).
[22] F. Baboux, F. Perez, C. A. Ullrich, I. D'Amico, G. Karczewski, and T. Wojtowicz, Phys. Rev. B **87**, 121303(R) (2013).
[23] Equation (19) differs from Eq. (15) in Ref. 9 by a factor $(\varepsilon_2 - \varepsilon_1)^2/\Omega_s^2$; for a detailed explanation see C. A. Ullrich, J. Chem. Theory Comput. **5**, 859 (2009).
[24] S. M. Badalyan, C. S. Kim, and G. Vignale, Phys. Rev. Lett. **100**, 016603 (2008).
[25] E. Ozbay, Science **311**, 189 (2006).
[26] J. F. Dobson, Phys. Rev. Lett. **73**, 2244 (1994).